



ELSEVIER

Contents lists available at [SciVerse ScienceDirect](http://SciVerse.Sciencedirect.com)

Computers & Geosciences

journal homepage: www.elsevier.com/locate/cageo

Computed 3D visualisation of an extinct cephalopod using computer tomographs

Alexander Lukeneder*

Natural History Museum Vienna, Geological–Palaeontological Department, Burgring 7, A-1010 Vienna, Austria

ARTICLE INFO

Article history:

Received 23 February 2012

Received in revised form

2 April 2012

Accepted 4 April 2012

Available online 13 April 2012

Keywords:

Computer tomography

3D visualisation

Palaeontology

Cephalopods

Cretaceous

ABSTRACT

The first 3D visualisation of a heteromorph cephalopod species from the Southern Alps (Dolomites, northern Italy) is presented. Computed tomography, palaeontological data and 3D reconstructions were included in the production of a movie, which shows a life reconstruction of the extinct organism. This detailed reconstruction is according to the current knowledge of the shape and mode of life as well as habitat of this animal. The results are based on the most complete shell known thus far of the genus *Dissimilites*. Object-based combined analyses from computed tomography and various computed 3D facility programmes help to understand morphological details as well as their ontogenetical changes in fossil material. In this study, an additional goal was to show changes in locomotion during different ontogenetic phases of such fossil, marine shell-bearing animals (ammonoids). Hence, the presented models and tools can serve as starting points for discussions on morphology and locomotion of extinct cephalopods in general, and of the genus *Dissimilites* in particular. The heteromorph ammonoid genus *Dissimilites* is interpreted here as an active swimmer of the Tethyan Ocean. This study portrays non-destructive methods of 3D visualisation applied on palaeontological material, starting with computed tomography resulting in animated, high-quality video clips. The here presented 3D geometrical models and animation, which are based on palaeontological material, demonstrate the wide range of applications, analytical techniques and also outline possible limitations of 3D models in earth sciences and palaeontology. The realistic 3D models and motion pictures can easily be shared amongst palaeontologists. Data, images and short clips can be discussed online and, if necessary, adapted in morphological details and motion-style to better represent the cephalopod animal.

© 2012 Elsevier Ltd. Open access under [CC BY-NC-ND license](http://creativecommons.org/licenses/by-nc-nd/4.0/).

1. Introduction

The creation of 3D models of fossils (e.g. cephalopods) helps visualising interpretation and may serve for mechanical models. 3D models of fossil specimens have become increasingly popular, providing more or less accurate reconstructions of volumes, spatial distribution, orientation and size of fossils in a sample as well as of biostratigraphic and diagenetic processes. Numerous complementary techniques have been advanced in recent years. These provide 3D datasets of palaeontological objects and involve both surface and volume scanning methods (e.g. microtomography). Laser scanning (airborne, terrestrial or desktop scanners) of surface morphology, point cloud data generated from digital images, or computed tomography down to a few microns (or even smaller) of spatial resolution are increasingly employed for geoscientific investigations, using an equally variable range of processing techniques and software packages. Numerous papers (e.g. Marschallinger, 2001; Maloof et al., 2010; Mayrhofer and

Lukeneder, 2010; Kruta et al., 2011; Marschallinger et al., 2011; Lukeneder and Lukeneder, 2011; Saupe et al., 2012) show the multitude of applications of 3D geometrical models in palaeontological studies. The great variability, the wide range of applications and the analytical techniques in the fossil record are demonstrated for dinosaurs (Rayfield et al., 2001, 2007; Balanoff et al., 2008; Witmer and Ridgely, 2009; Fortuny et al., 2011; Tsuihiji et al., 2011; Knoll et al., 2012), lizards (Polcyn et al., 2002), birds (Rowe et al., 2001; Degrange et al., 2010; Zelenitsky et al., 2011), fishes (Gai et al., 2011), mammals (Luo et al., 2002), molluscs (Hoffmann and Zachow, 2011), brachiopods (Gaspard et al., 2011), plants (Friis et al., 2007; Scott et al., 2009), algal or acritarch fossils (Cunningham et al., 2012), and protists (Donoghue et al., 2006; Dong et al., 2010; Hultgren et al., 2011). The latter papers also outline possible limitations of 3D models in earth sciences and in palaeontology.

The main goal of this paper is to present methods and possibilities for visualisation of palaeontological material based on computed tomography and palaeontological features (e.g., morphology; Fig. 1). Using computer facilities such as Nurbs Realtime Editor, CAD Application Rhinoceros[®] 4.0, Model Editor, 3d Studio Max[®] from Autodesk[®] or 3D Coat[®] yield a more

* Tel.: +43 1 52177 251; fax: +43 1 52177 459.

E-mail address: alexander.lukeneder@nhm-wien.ac.at

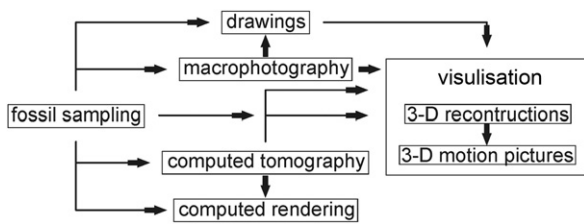


Fig. 1. Principal steps in 3D visualisation of palaeontological material such as fossil cephalopods.

detailed picture of the morphology of the genus *Dissimilites* and its swimming habits. The result is the computed 3D model of the fossil cephalopod *Dissimilites* itself along with the reconstruction of a 3D model in the framework of motion pictures showing animated animals in their habitat. A 3-year project of the Austrian Science Fund (FWF P20018-N10) resulted in accurate reconstructions of cephalopods and demonstrated the increasing importance of 3D models in palaeontology.

2. Morphological details obtained by computed tomography

Noninvasive techniques allow to process great volumes of information, detected by computer tomography on fossils material, without causing any alteration. The tomography scans were made at the Upper Austria University of Applied Science in Wels. The 3D computed tomography (CT) device RayScan 250 E is a 3D CT system with two X-ray sources (a 225 kV micro-focus and a 450 kV mini-focus X-ray tube) for the inspection of a wide variety of parts, ranging from micro-objects (high resolution) to macroscopic ones (large penetration length). The system is additionally equipped with a 2048 × 2048 pixels flat-panel detector; it absorbs energy of the X-rays and reemits the absorbed energy in the form of light, which can be detected. In the case of an industrial CT-system, the specimen is rotated by 360° and at each pre-defined angle step a 2D-projection image is captured. The complete set of projection images is then reconstructed to 3D volume data using a mathematical algorithm. The data consists of volumetric pixels (voxels), whose size limits the detail detectability. For each fossil part, the optimal voxel size and tube voltage were set according to the specimen's dimensions. A more detailed introduction to computed tomography is beyond the scope of this article. For the details of X-ray computed tomography as a technique of imaging and quantification of internal features of sediments and fossils see Mees et al. (2003). The non-destructive CT provides the basal information on morphological features of the respective fossil cephalopod.

3. Palaeontological material

The shape data derived from a recently described species, namely *Dissimilites* nov. sp. (Lukeneder and Lukeneder, in press; Fig. 2). This fossil cephalopod originates from the Puez locality (Dolomites, northern Italy). The material was collected within the FWF project P20018-N10 and is stored at the Natural History Museum in Vienna (NHMW, holotype 2012/0002/0001). The heteromorph ammonoid was collected by Susanne Lukeneder from Lower Barremian beds (approx. 127 million years old) at the Puez section.

The outcrop is situated on the Puez-Odle-Gardenaccia Plateau in the Dolomites (maps Trentino—Alto Adige; South Tyrol; Lukeneder, 2010). The exact position is about 30 km northeast

of Bozen (E 011°49'15", N 46°35'30"; Lukeneder, 2010,2012, 2012). A detailed description of the geology and lithostratigraphy is given in Lukeneder (2010).

4. Visualisation and motion pictures

4.1. Macrophotography

Detailed images of the specimen were taken with a Kodak Professional DCS Pro combined with the photo device Stereo Discovery V20 with AxioCam MR5 Zeiss. All images have the same file structure with *Dissimilites.tiff*, 600 dpi resolution. Black-and-white images are combined with full colour images for high visibility of fossil edges and details (Fig. 2).

4.2. Computed tomography

3D computed tomography was performed at a 225 kV micro-focus and a 450 kV mini-focus X-ray tube. The specimen and the embedding fossiliferous marly limestone were tomographed frontally and axially (angle of 90°; Figs. 2 and 3). Frontal and axial slice-images were animated to videos as *frontal.avi* and *axial.avi* motion pictures. 654 frontal slices (000.jpg-654.jpg; 342 MB) with 0.11 mm/pixel space and 1 619 axial slices (0000.jpg-1619.jpg, 376 MB) with 0.11 mm/pixel space were produced. Measurements were performed with durations of 56, 68 and 92 min. Voxel sizes were 95 and 75.01 μm. Electrical voltage was at 220 and 400 kV with 425 and 1500 μA. Exposure time was at 600, 999, and 2000 ms. 1440 projections with a Cu pre-filter 1.0, 2.0 and 4.0 mm were made. Additionally, the surface (e.g., stone vs. air) was rendered to image the cephalopod's morphology (Fig. 3f).

4.3. 3D visualisation and motion pictures of fossil cephalopods

The modelling procedure of the fossil cephalopod is based on line drawings on which successive cross-sections were fitted. Additionally, the series of CT images turned out to be an essential source to understand the fossil's morphology and shape. Both were used to draw the cross-sections used in the later-processed 3D model. The images present a grey scale spectrum which was further refined by converting its height information, ranging from darker to lighter areas, to a so-called "Normal Map" image. This helped to refine the visual appearance and understand various delicate structures. The process involved projecting this Normal Map onto a surface inside a 3D Realtime Editor and then introducing a virtual light source, which was tilted in different directions to gain plasticity from highlights and shadows (Fig. 3).

The 3D modelling procedure was carried out in different stages using different 3D modelling and animation software facilities and programmes (e.g., Nurbs Realtime Editor, Model Editor or 3d Studio Max[®] from Autodesk[®]), each specialized for its defined task. The first step was to achieve a precise volume model of the fossil cephalopod, followed by refining its geometric shape by adjusting scale and patterns to place the discrete spines. The final texture was created by colouration and image information directly on its surface in preparation for the final rendering and animation process (Fig. 4).

The outline of *Dissimilites intermedius* was vectorised and imported into a CAD Application (Rhino[®] 4.0), which is orientated to create 3D geometry from so-called NURBS (Non Unified Rational B-Splines), and hereafter used as a guideline to extrude the prepared cross-sections along its edges. Various other techniques had been tested before, including the manual

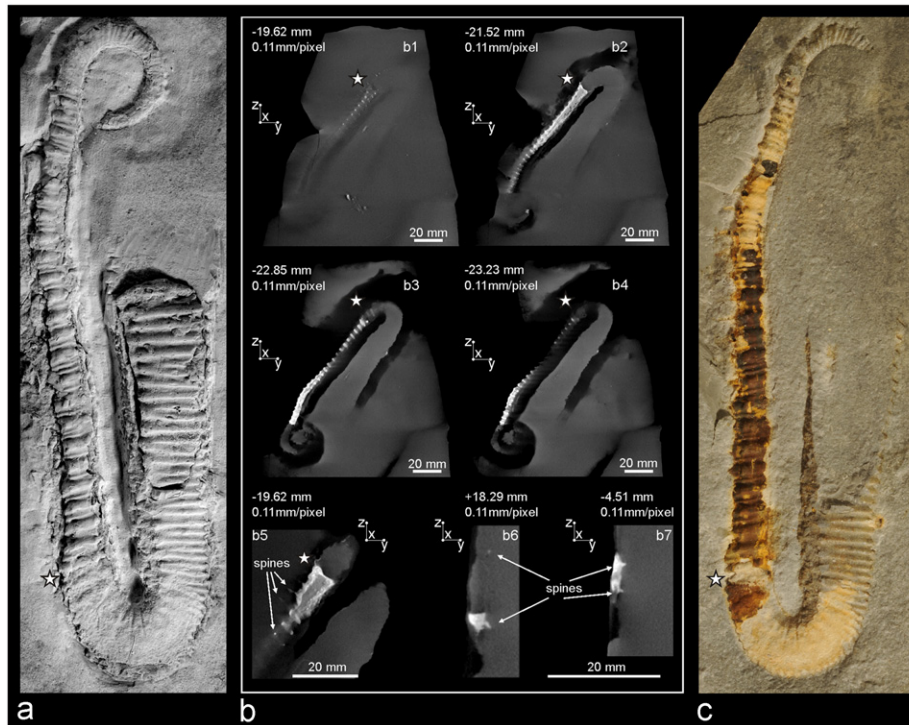


Fig. 2. (a) *Dissimilites* specimen coated with ammonium chloride (600 dpi). Asterisk marks the beginning of body chamber, (b) computed tomography slices from the specimen (due to the limonitic preservation in white) and the embedding limestone (grey). Performed on a RayScan 250 E, with a 450 kV mini-focus X-ray tube and a 2048×2048 pixel flat panel detector (cone beam reconstruction), (b1–b5) frontal slices and (b6–b7) axial slices. Slice spacing is 0.11 mm/pixel space, (c) image of *Dissimilites* uncoated with limonitic preservation (yellow to orange, 600 dpi). (For interpretation of the references to colour in this figure legend, the reader is referred to the web version of this article.)

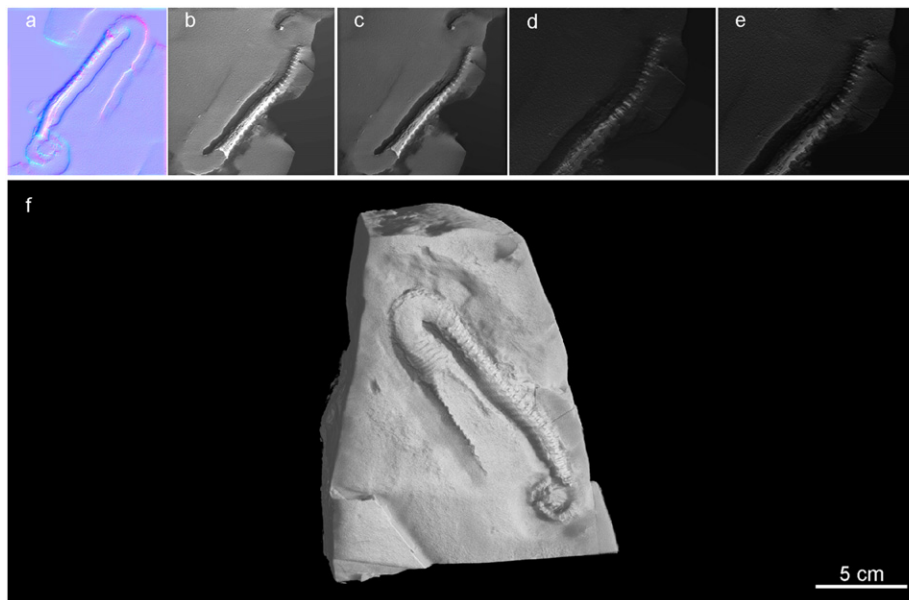


Fig. 3. (a–e) Normal Map and visualisation onto a surface inside a 3D Realtime Editor. Virtual light source was tilted in different directions to gain plasticity from highlights and shadows, (f) rendered surface model based on data from a RayScan 250 E, with a 450 kV mini-focus X-ray tube. Spacing of rendered slices is 0.11 mm/pixel space (600 dpi).

extrusion of the sections or their replication, but with unsatisfactory results.

To refine surface features, the NURBS Model was brought into 3D Studio Max[®] from Autodesk[®]. The detailed morphology

features visible on the macrophotographs and CT images of the source material were used to determine the size and location of ribs and spines. These were then modelled and placed by hand. The soft tissue of the cephalopod animal was processed by

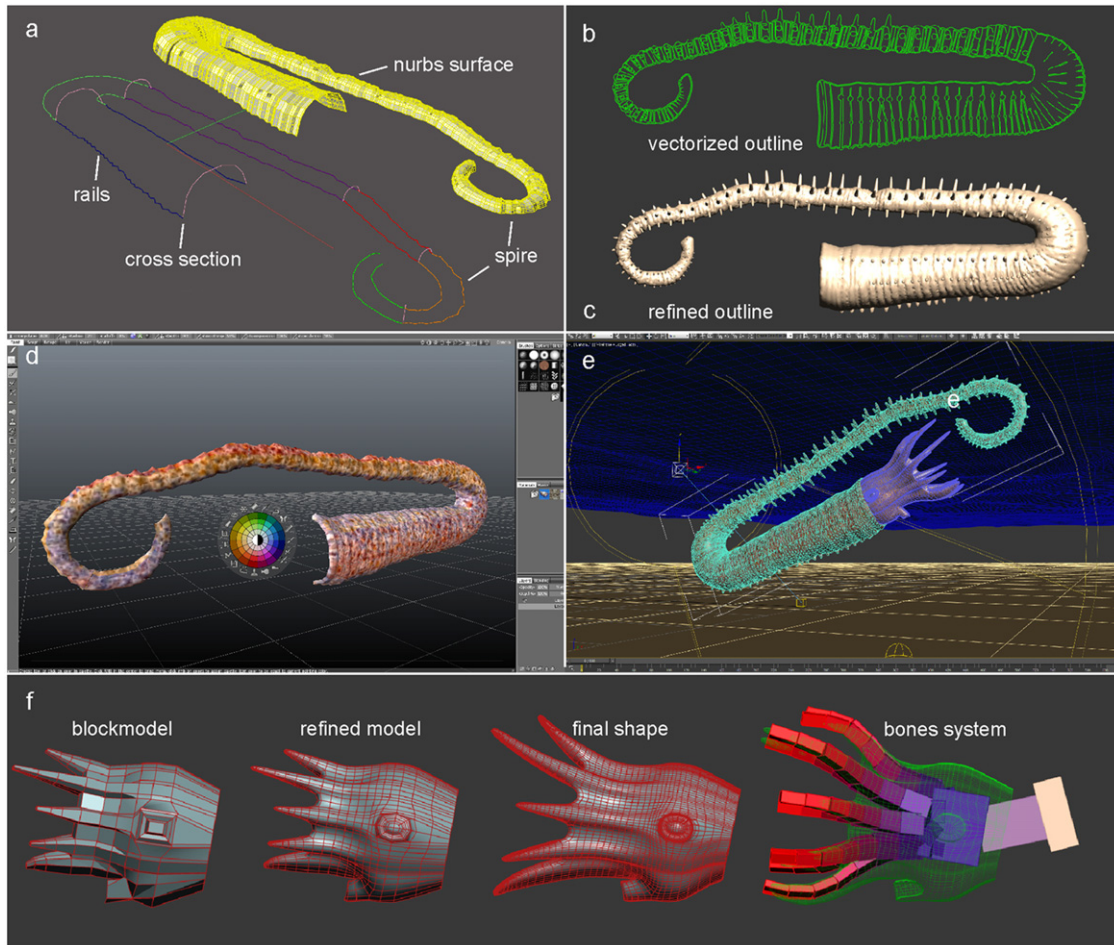


Fig. 4. (a) Visualisation by final rendering in *Nurbs Model Editor* and *3d Studio Max*® by Michael Klein (7reasons), (b–c) vectorisation and geometrical refinement in *3D Studio Max*, (d) imported geometries with paint application tools, (e) scene setup for the final rendering in *3D Studio Max*, (f) modelling process in the Kinematic Bone System.

3D Studio Max®, starting with a basic shape, which was subsequently refined by precision of morphological characters (Fig. 4). It has to be noted that not much is known on soft parts of ammonites (Lehmann, 1990; Maeda and Seilacher, 1996), their habitats (Jacobs et al., 1994a,b; Westermann, 1996; Lukeneder et al., 2010), and the locomotion of fossil cephalopods (Jacobs, 1992, 2001; Jacobs and Chamberlain, 1996; Monks and Young, 1998; Klug and Korn, 2004).

The resulting geometries were exported to an additional programme specialized in 3D texturing and painting (*3D Coat*®). UVW mapping allows direct painting on the 3D surface of the generated models. UVW describes the coordinates of the underlying mesh in its *x*-, *y*-, and *z*-axis and translates a given texture or coloration to distinct areas or morphological features. For the actual process of painting, various maps were gathered from existing images and placed in the background of the application; the 3D model was placed in front, and parts of these images were projected onto a special marked area.

The final geometries were then re-imported to *3D Studio Max*® for the animation and rendering setup (Fig. 4). For the animation of the animal's body, virtual "elements" were created by the inverse kinematic bones system and linked to a hierarchy with inverse kinematic constraints (Fig. 4f). This allows the animator to move several bones by using only the last link of this hierarchy. The surrounding scenery was assembled with a simple plane for the sea floor, a parametric geometry serving as a water plane, and the setting of virtual

lights and ambient influences (e.g., lights through waves; Fig. 5; Animation 1).

4.4. 3D visualisation of ontogenetical stages in *Dissimilites*

Although the presented animation is based on the best preserved and most complete specimen known, the embryonic stage is still unknown (Lukeneder and Lukeneder, in press). The successive ontogenetical stages are separated into a juvenile, mid-age and adults stage (Fig. 5). Morphological terms and ontogenetical stages are in accordance to terms used by Westermann (1996), Lukeneder et al. (2010), and Lukeneder and Lukeneder (in press). The mid-aged stage herein is equivalent to the preadult stage of Klug (2001).

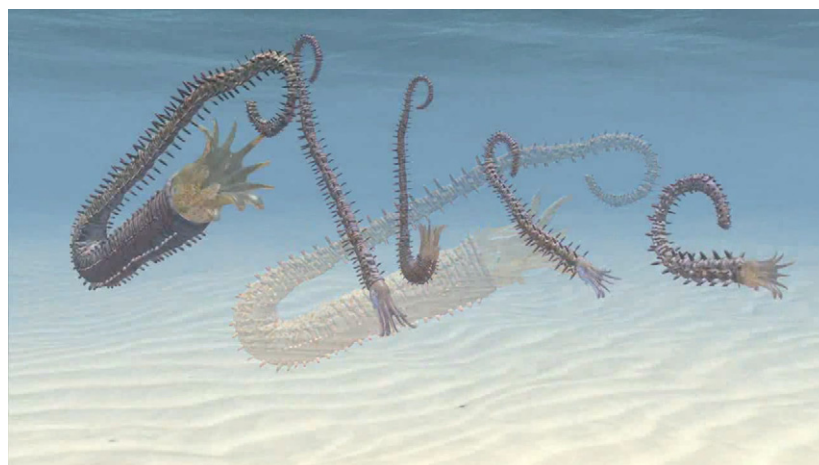
The resulting 3D reconstruction of ontogenetical stages in the fossil cephalopod *Dissimilites* appear with the juvenile cyrtocone animal (Fig. 5a), the mid-aged animal with straight shell (Fig. 5b–c) followed later by a short hook (Fig. 5d), and different views of the final, adult animal (Fig. 5e–h). The adult stage is characterised by a long, prominent hook (e.g. ancylocone) and the last change in swimming position (Animation 1).

5. Conclusions

The study presents results of an object-based combined analysis from computed tomography and various computed 3D



Fig. 5. (a–h) 3D reconstruction of successive ontogenetic stages in the fossil cephalopod *Dissimilites* (600 dpi). (a) Cyrtocone juvenile animal. (b–d) Mid-aged animal with straight shell stages. (e–h) Different views of the adult, mature animal.



Animation 1. Representative frame still (timeslice at sec. 18) from the attached 3D animation (*Dissimilites*.mp4; 11.1 MB) of the Cretaceous cephalopod *Dissimilites* in different ontogenetic stages and its habitat. Animation is inspired from data for shell orientation in Cretaceous heteromorph ammonoids according to Kakabadzé and Sharikadzé (1993), Monks and Young (1998), Kaplan (2002). The animation will be linked with the data library PANGAEA (www.pangaea.de). Supplementary material related to this article can be found online at <http://dx.doi.org/10.1016/j.cageo.2012.04.003>.

facility programmes performed on the most complete shell of the fossil cephalopod *Dissimilites*. The first 3D visualisation of the heteromorph cephalopod genus *Dissimilites* from the Southern Alps (Dolomites, northern Italy) is presented. Based on the morphological changes, equivalent with changes in growth stages (e.g. ribbing, morphology and direction of shell), successive ontogenetical stages were reconstructed. Three ontogenetical stages can be separated in *Dissimilites* with juvenile, mid-aged and adult animals. A cyrticone juvenile stage is followed by a straight conch, and the adult, mature stage is hooked, simultaneously accompanied by a change of swimming position. Computed tomography and palaeontological data are combined with 3D reconstructions, yielding a movie. This case study demonstrates the non-destructive possibilities of 3D visualisation for palaeontological material. The resulting images are quite realistic, and a short animated clip showing the morphology and motion of the animal is the first in such high quality using palaeontological material. The realistic 3D models and motion pictures can be simply shared amongst palaeontologists. Data, images and short-clips can be discussed online and adapted morphologically or with regard to the cephalopod's motion.

Acknowledgements

The work on this material has been sponsored by the Austrian Science Fund (FWF, Project P20018-N10). Sincere thanks go to Christian Gusenbauer (Wels) for performing the computer tomography. Michael Klein from the 7reasons Media Agency (Vienna) was responsible for the visualisation and animation. The author appreciates the suggestions and comments of Christian Klug (Zurich) and the editors of Computers and Geosciences which improved the quality of the manuscript. Macrophotographs were taken by Alice Schumacher (Vienna).

References

- Balanoff, A.M., Norell, M.A., Grellet-Tinner, G., Lewin, M.R., 2008. Digital preparation of a probable neoceratopsian preserved within an egg, with comments on microstructural anatomy of ornithischian eggshells. *Naturwissenschaften* 95, 493–500.
- Cunningham, J.A., Thomas, C.W., Bengtson, S., Kearns, S.L., Xiao, S., Marone, F., Stampanoni, M., Donoghue, P.C.J., 2012. Distinguishing geology from biology in the Ediacaran Doushantuo biota relaxes constraints on the timing of the origin of bilaterians. *Proceedings of the Royal Society B: Biological Sciences* <http://dx.doi.org/10.1098/rspb.2011.2280>.
- Degrange, F.J., Tambussi, C.P., Moreno, K., Witmer, L.M., Wroe, S., 2010. Mechanical analysis of feeding behavior in the extinct “terror bird” *Andalgalornis steulleti* (Gruiformes: Phorusrhacidae). *PLoS ONE* 5 (8), e11856, <http://dx.doi.org/10.1371/journal.pone.0011856>.
- Dong, X.P., Bengtson, S., Gostling, N.J., Cunningham, J.A., Harvey, T.H.P., Kouchinsky, A., Val'kov, A.K., Repetski, J.E., Stampanoni, M., Marone, F., Donoghue, P.C.J., 2010. The anatomy, taphonomy, taxonomy and systematic affinity of Markueilia: Early Cambrian to Early Ordovician scalidophorans. *Palaentologia* 53/6, 1291–1314.
- Donoghue, P.C.J., Bengtson, S., Xi-ping, D., Gostling, N.J., Huldgren, T., Cunningham, J.A., Yin, C., Yue, Z., Peng, F., Stampanoni, M., 2006. Synchrotron X-ray tomographic microscopy of fossil embryos. *Nature* 442, 680–683.
- Fortuny, J., Galobart, A., De Santisteban, C., 2011. A new capitosaur from the Middle Triassic of Spain and the relationships within the Capitosauria. *Acta Palaentologica Polonica* 56/3, 553–566.
- Friis, E.M., Crane, P.R., Pedersen, K.R., Bengtson, S., Donoghue, P.C.J., Grimm, G.W., Stampanoni, M., 2007. Phase-contrast X-ray microtomography links Cretaceous seeds with Gnetales and Bennettitales. *Nature* 450, 549–552.
- Gai, Z., Donoghue, P.C.J., Zhu, M., Janvier, P., Stampanoni, M., 2011. Fossil jawless fish from China foreshadows early jawed vertebrate anatomy. *Nature* 08/2011 (476), 324–327.
- Gaspard, D., Putlitz, B., Baumgartner, L., 2011. X-ray computed tomography—a promising tool for brachiopod shell investigations. *Proceedings IAMG 2011 Salzburg* 2011, 518–533.
- Hoffmann, R., Zachow, S., 2011. Non-invasive approach to shed new light on the buoyancy business of chambered cephalopods (Mollusca). *Proceedings IAMG 2011 Salzburg*, 507–517.
- Huldgren, T., Cunningham, J.A., Yin, C., Stampanoni, M., Marone, F., Donoghue, P.C.J., Bengtson, S., 2011. Fossilized Nuclei and Germination Structures Identify Ediacaran “Animal Embryos” as Encysting Protists. *Science* 334, 1696–1699.
- Jacobs, D.K., 1992. Shape, drag, and power in ammonoid swimming. *Paleobiology* 18, 203–220.
- Jacobs, D.K., 2001. Buoyancy, dynamics and structure in chambered cephalopods. In: Briggs, D.E.G., Crowther, P. (Eds.), *Palaebiology II*. Blackwell Science, Oxford, pp. 397–401.
- Jacobs, D.K., Landman, N.H., Chamberlain, J.A., 1994a. Ammonite shell shape covaries with facies and hydrodynamics: iterative evolution as a response to changes in basin environment. *Geology* 22/10, 905–908.
- Jacobs, D.K., Landman, N.H., Chamberlain, J.A., 1994b. Buoyancy and Hydrodynamics in Ammonoids. In: Landmann, N.H., Tanabe, K., Davis, R.A. (Eds.), *Ammonoid Paleobiology, Topics in Geobiology*, 13. Plenum, New York, pp. 169–224.
- Jacobs, D.K., Chamberlain, J.A., 1996. Buoyancy and hydrodynamics in ammonoids. In: Landman, N.H., Tanabe, K., Davis, R.A. (Eds.), *Ammonoid Paleobiology, Topics in Geobiology*, Plenum, New York, pp. 169–223.
- Kakabadzė, M.V., Sharikadzė, M.Z., 1993. On the mode of life of heteromorph ammonites (heterocone, ancylocone, ptychocone). *Geobios* 15, 209–215.
- Kaplan, P., 2002. Biomechanics as a test of functional plausibility: testing the adaptive value of terminal-countdown heteromorph in Cretaceous ammonoids. In: Summesberger, H., Histon, K., Daurer, A. (Eds.), *Cephalopods Present and Past*, 57. *Abhandlungen der Geologischen Bundesanstalt*, pp. 181–197.
- Klug, C., 2001. Life-cycles of some Devonian ammonoids. *Lethaia* 34, 215–233.
- Klug, C., Korn, D., 2004. The origin of ammonoid locomotion. *Acta Palaentologica Polonica* 49/2, 235–242.
- Knoll, F., Witmer, L.M., Ortega, F., Ridgely, R.C., Schwarz-Wings, D., 2012. The braincase of the basal Sauropod Dinosaur *Spinophorosaurus* and 3D reconstructions of the cranial endocast and inner ear. *PLoS ONE* 7 (1), e30060, <http://dx.doi.org/10.1371/journal.pone.0030060>.
- Kruta, I., Landman, N., Rouget, I., Cecca, F., Tafforeau, P., 2011. The role of ammonites in the Mesozoic marine food web revealed by jaw preservation. *Science* 331/6013, 70–72.
- Lehmann, U., 1990. *Ammonoideen*. Haeckel Bücherei, Enke Verlag, Stuttgart, 1–257.
- Lukeneder, A., 2010. Lithostratigraphic definition and stratotype for the Pueze Formation: Formalization of the Lower Cretaceous in the Dolomites (S. Tyrol, Italy). *Austrian Journal of Earth Sciences* 103/1, 138–158.
- Lukeneder, S., Lukeneder, A., 2011. Methods in 3D modelling of Triassic Ammonites from Turkey (Taurus, FWF P22109-B17). *Proceedings IAMG 2011 Salzburg*, 496–505, <http://dx.doi.org/10.5242/iamg.2011.0225>.
- Lukeneder, A., 2012. New biostratigraphic data on an Upper Hauterivian/Upper Barremian ammonite assemblage from the Dolomites (Southern Alps, Italy). *Cretaceous Research* 35, 1–21.
- Lukeneder, A., Lukeneder, S., in press. A new species of the Barremian (Cretaceous) heteromorph ammonite genus *Dissimilites* of northern Italy. *Acta Palaentologica Polonica*.
- Lukeneder, A., Harzhauser, M., Müllegger, S., Piller, W.E., 2010. Ontogeny and habitat change in Mesozoic cephalopods revealed by stable isotopes ($\delta^{18}\text{O}$, $\delta^{13}\text{C}$). *Earth and Planetary Science Letters* 296, 103–114.
- Luo, Z.X., Kielan-Jaworowska, Z., Cifelli, R.L., 2002. In quest for a phylogeny of Mesozoic mammals. *Acta Palaentologica Polonica* 47, 1–78.
- Maeda, H., Seilacher, A., 1996. Ammonoid taphonomy. In: Landmann, N.H., Tanabe, K., Davis, R.A. (Eds.), *Ammonoid Paleobiology, Topics in Geobiology*, 13. Plenum, New York, pp. 543–578.
- Maloof, A.C., Rose, C.V., Beach, R., Samuels, B.M., Calmet, C.C., Erwin, D.H., Poirier, G.R., Yao, N., Simons, F.J., 2010. Possible animal-body fossils in pre-Marinoan limestones from South Australia. *Nature Geoscience* 3, 653–659.
- Marschallinger, R., 2001. Three-dimensional reconstruction and visualization of geological materials with IDL—examples and source code. *Computers & Geosciences* 27 (4), 419–426.
- Marschallinger, R., Hofmann, P., Daxner-Höck, G., Ketcham, R.A., 2011. Solid modeling of fossil small mammal teeth. *Computers & Geosciences* 37 (9), 1364–1371.
- Mayrhofer, S., Lukeneder, A., 2010. In: Marschallinger, R., Wanker, W., Zobl, F. (Eds.), *3D Modellierung eines Karnischen Ammoniten Massenvorkommens (Taurus, Türkei; FWF P22109 B17)*, 2010. *Beiträge zur COGeo*, pp. 12, <http://dx.doi.org/10.5242/cogeo.2010.0000>.
- Mees, F., Swennen, R., Van Geet, M., Jacobs, P., 2003. Applications of X-ray Computed Tomography in the Geosciences. *Special Papers of the Geological Society, London*, 215, 1–243.
- Monks, N., Young, A.R., 1998. Body and the functional morphology of Cretaceous heteromorph ammonites. *Palaentologia Electronica* 1 (1) <<http://www-odp.tamu.edu/paleo/toc.htm>>.
- Polcyn, M.J., Rogers, J.V., Kobayashi, Y., Jacobs, L.L., 2002. Computed tomography of an Anolis lizard in Dominican amber: systematic, taphonomy, biogeography, and evolutionary implications. *Palaentologia Electronica* 5 (1) <http://paleo-electronica.org/paleo/2002_1/amber/issue1_02.htm>.
- Rayfield, E.J., Norman, D.B., Celeste, C., Horner, C.C., Horner, J.R., Smith, P.M., Jeffrey, J., Thomason, J.J., Upchurch, P., 2001. Cranial design and function in a large theropod dinosaur. *Nature* 409, 1033–1037.
- Rayfield, E.J., Milner, A.C., Xuan, V.B., Yound, P.G., 2007. Functional morphology of spinosaur ‘crocodile-mimic’ dinosaurs. *Journal of Vertebrate Paleontology* 27, 892–901.

- Rowe, T., Ketcham, R.A., Denison, C., Colbert, M., Xu, X., Currie, P.J., 2001. Forensic palaeontology—the *Archaeoraptor* forgery. *Nature* 410, 539–540.
- Saupe, E.E., Fuente, R.P., Selden, P.A., Delclos, X., Tafforeau, P., Soriano, C., 2012. New *Orchestina* Simon, 1882 (Araneae: Oonopidae) from Cretaceous ambers of Spain and France: first spiders described using phase-contrast X-ray synchrotron microtomography. *Palaeontology* 55 (1), 127–143.
- Scott, A.C., Galtier, J., Gostling, N.J., Smith, S.Y., Collinson, M.E., Stampanoni, M., Marone, F., Donoghue, P.C.J., Bengtson, S., 2009. Scanning electron microscopy and synchrotron radiation X-Ray tomographic microscopy of 330 million year old charcoalfied seed fern fertile organs. *Microscopy and Microanalysis* 15, 166–173.
- Tsuihiji, T., Watabe, M., Tsogtbaatar, K., Tsubamoto, T., Barsold, R., Suzuki, S., Lee, A.H., Ridgely, R., Kawahara, Y., Witmer, L.M., 2011. Cranial osteology of a juvenile specimen of *Tarbosaurus bataar* (Theropoda, Tyrannosauridae) from the Nemegt Formation (Upper Cretaceous) of Bugin Tsav, Mongolia. *Journal of Vertebrate Paleontology* 31 (3), 497–517.
- Westermann, G.E.G., 1996. Ammonoid life and habitat. In: Landman, N., Tanabe, K., Davis, R.A. (Eds.), *Ammonoid Paleobiology*. Topics in Geobiology, 13. Plenum, New York, pp. 607–707.
- Witmer, L.M., Ridgely, R.C., 2009. New insights into the brain, braincase and ear region of Tyrannosaurs (Dinosauria, Theropoda), with implications for sensory organization and behaviour. *The Anatomical Record* 292, 1266–1296.
- Zelenitsky, D.K., Therrien, F., Ridgely, R.C., McGee, A.R., Witmer, L.M., 2011. Evolution of olfaction in non-avian dinosaurs and birds. *Proceedings of the Royal Society B* 278, 3625–3634.